Electrical Relaxation of Bismuth Germanate Silicate Glasses

Y. H. Rim,[†] B. S. Lee,[†] H. W. Choi,[‡] J. H. Cho,[‡] and Y. S. Yang*,[‡]

School of Liberal Arts, Semyung University, Chechon, Chungbuk 390-711, Korea, and School of Nano Science and Technology, RCDAMP, Department of Physics, Pusan National University, Pusan 609-735, Korea

Received: January 20, 2006; In Final Form: March 7, 2006

The frequency-dependent electrical data of the bismuth germanate silicate (BGSO) glasses have been discussed in the framework of the electric modulus representation and the power-law conductivity. The activation energies of the mean electric relaxation time and the direct current (dc) conductivity obtained by the complex modulus analysis show that the BGSO glasses satisfy the Barton, Nakajima, and Namikawa (BNN) relation. The proper relation between the exponent of the power-law conductivity and the stretched exponential of the modulus representation is shown. The temperature- and frequency-dependent characteristics of non-Debye behavior are discussed. The scaling properties of both the modulus $M^*(\omega)$ and the alternating current (ac) conductivity $\sigma^*(\omega)$ are examined.

I. Introduction

Heavy metal oxide cations in the traditional glass formers such as silicate and germanate have been proposed as candidates for the scintillation detector because of their high stopping power and medical imagery that have long been known. Bismuth germanate $Bi_4Ge_3O_{12}$(BGO) and bismuth silicate $Bi_4Si_3O_{12}$ (BSO) crystals are synthetic materials having an eulytite structure. These crystals are attractive because of their electro-optical, electromechanical, and intense luminescence properties, the short wavelength of radiation, laser materials when doped with rare earths, and the fact that they are nonhygroscopic.[1−3] In particular, BGO has received a lot of attention because of its uses as a scintillator, in X-ray and positron emission tomography, and telescopes for hard X- and γ-rays in astrophysics and nuclear physics. Even though many studies on the ionic conductivity and relaxation in oxide glasses have been reported,[4−10] there has been a lack of a temperature- and frequency-dependent dielectric studies on the bismuth germanate silicate glasses.

Electrical conductivity relaxation measurements of diffusing ions in glasses, melts, and crystals are most often analyzed in the context of either the real part of the complex conductivity, $\mathrm{Re}[\sigma^*(\omega)]$, or the complex electric modulus, $M^*(\omega)$.[4−10]

In a previous paper,[11] we studied the conductivity mechanism in $Bi_4(Ge_xSi_{1-x})_3O_{12}$ (BGSO) glasses at various temperatures, where $x = 0$, 0.33, 0.66, and 1. Then the complex impedance Cole−Cole plot and the power-law method were adapted for the analysis of the electrical conductivities of direct current (dc) and alternating current (ac), and the Barton, Nakajima, and Namikawa (BNN) relation was examined.

In this paper, we present the results of the analysis of the complex modulus representation with the Kohlrausch−Williams−Watts (KWW) distribution for the BGSO glasses and then characterize the dynamics of the electric relaxation of our samples by comparing them with the results of the power-law ac conductivity representation, which is the extended study of Yang et al.[11]

We have found a proper relation between the power-law exponent n of the ionic conducting glass conductivity and the stretching exponent β of the KWW function by solving the macroscopic conductivity, $\sigma^*_{EM}(\omega)$, which is obtained from the electric modulus formalism via the Maxwell relation. The appropriate choice of scaling factors for the ac conductivity and electric modulus of BGSO glasses are introduced.

II. Experimental Section

Glasses of $2Bi_2O_3$-$3[xGeO_2$-$(1-x)SiO_2]$, with $x = 0$, 0.33, 0.66, and 1, were prepared by melting crystalline powders in a cylindrical electric furnace at 1423 K in air through a twin roller, in which the estimated cooling rate was about 10^5 K/s.

In this study, we simplify the notations according to the Ge/Si atomic ratio. They are $Bi_4Ge_3O_{12}$≡BGO, $Bi_4Ge_2Si_1O_{12}$≡BGSO21, $Bi_4Ge_1Si_2O_{12}$≡BGSO12, $Bi_4Si_3O_{12}$≡BSO, and $Bi_4(Ge_xSi_{1-x})_3O_{12}$≡BGSO.

X-ray diffraction (XRD), differential scanning calorimetry (DSC), scanning electron microscopy (SEM), and Raman spectroscopy measurements were conducted to investigate the crystallization process.[12] The glass transition temperature, T_g, and the crystallization temperature, T_c, were determined as the points where the DSC curves depart from the horizontal baselines and meet with an extrapolation at inflections of the thermal chord,[12] which were shown in the previous paper. The as-quenched glass was measured by DSC to determine T_g and the supercooled liquid region.

Measurements of the complex impedance were performed over a linear frequency range from 100 Hz to 15 MHz for the temperature range 300−923 K with the heating rate of 2 K/min using a commercial impedance/gain-phase analyzer (Hewlett-Packard LF4194A, U.S.). The parallel surfaces of the sample of thickness 0.1 mm and diameter ~8.8 mm were coated by vacuum evaporation with gold for electrodes.

III. Results and Discussion

A. Electric Modulus Representation. The complete characterization of the non-Debye dielectric relaxation in complex heterogeneous materials such as ionic conducting glasses, composite materials, polymers, biological cells, porous materials,

* To whom correspondence should be addressed. Tel: 82-51-510-2958. Fax: 82-51-516-5682. E-mail: ysyang@pusan.ac.kr.
[†] Semyung University.
[‡] Pusan National University.

10.1021/jp060415s CCC: $30.25
Published on Web 04/01/2006

and liquid crystals requires the use of a variety of techniques to span the relevant ranges in frequency. That is, the Havriliak−Negami (HN)[13−15] relationship, the Mittag−Leffler series expansion function,[16,17] and the fractional dynamics[14,18,19] have been used to describe the non-Debye dielectric spectrums. All of these functions use two free parameters to determine the dielectric response. However, we choose single parameter representation concerning the frequency and relaxation time to describe the dielectric response of the ionic conducting glasses.

Here, we adopt the modulus representation to study the frequency-dependent conductivity of BGSO glasses. The complex modulus $M^*(\omega)$ is applied to materials with nonzero dc conductivity by Moynihan et al.[20−23] and $M^*(\omega)$ is simply related to $\sigma^*(\omega)$ via

$$M^*(\omega) = 1/\epsilon^*(\omega) = i\omega\epsilon_0/\sigma^*(\omega) \quad (1)$$

In the frequency domain, the complex electric modulus $M^*(\omega)$ is defined by

$$M^*(\omega) = M'(\omega) + iM(\omega) = M_\infty[1 - \int_0^\infty \mathrm{d}t \exp(-i\omega t)(-\mathrm{d}\phi(t)/\mathrm{d}t)] \quad (2)$$

where ϵ^* ($= \epsilon' - i\sigma'/\omega\epsilon_0$) is the complex permittivity, ϵ' and σ' the real parts of the complex permittivity and of the complex conductivity, respectively, ω angular frequency, ϵ_0 the permittivity of a vacuum, M_∞ the limiting high-frequency value of M', and $\phi(t)$ an electric field relaxation function in the time domain.

It has long been realized that the stretched-exponential function or Kohlrausch−Williams−Watts (KWW) function[24,25]

$$\phi(t) = \exp[-(t/\tau_k)^\beta] \quad 0 < \beta \leq 1 \quad (3)$$

provides a reasonable fit to typical experimental data with a single parameter in the electric modulus representation.[20−23] Here, β is a stretching exponent, tending to unity for a Debye type of relaxation, and τ_k is the KWW relaxation time related to $\langle\tau\rangle$ by the expression[20]

$$\langle\tau\rangle \equiv \int_0^\infty \mathrm{d}t\phi(t) = \tau_k\Gamma(1/\beta)/\beta \quad (4)$$

where Γ denotes the gamma function and $\langle\tau\rangle$ is the mean electric relaxation time. The solid curves in Figure 1 are the best fits to eq 2 with the KWW function.

The frequency dependence of $M'(\omega)$ and $M''(\omega)$ for BGO glass at various temperatures is shown in Figure 1. $M'(\omega)$ and $M''(\omega)$ exhibit the dispersion characteristics of a relaxation process. $M'(\omega)$ shows a dispersion tending to M_∞ at higher frequencies, while a broad $M''(\omega)$ exhibits an asymmetric maximum, M''_{max}. The peak frequency ω_m corresponding to M''_{max} gives the most probable relaxation time or the mean electric field relaxation time, $\langle\tau\rangle$, from the condition $\omega_m\langle\tau\rangle = 1$.[22] The position of the peak of $M''(\omega)$ at ω_m shifts to higher frequencies as the temperature increases, indicating that the system stabilizes in a short time for an external force at elevated temperature.

In Figure 2, we present the variation of the peak frequency ω_m, obtained from the imaginary part of the complex modulus plot, with reciprocal temperature for various compositions of BGSO glasses. The figure shows that the peak frequency obeys the Arrhenius relation $\omega_m = \omega_0 \exp(-E_m/kT)$, where E_m is the activation energy from the complex modulus plot and k is the

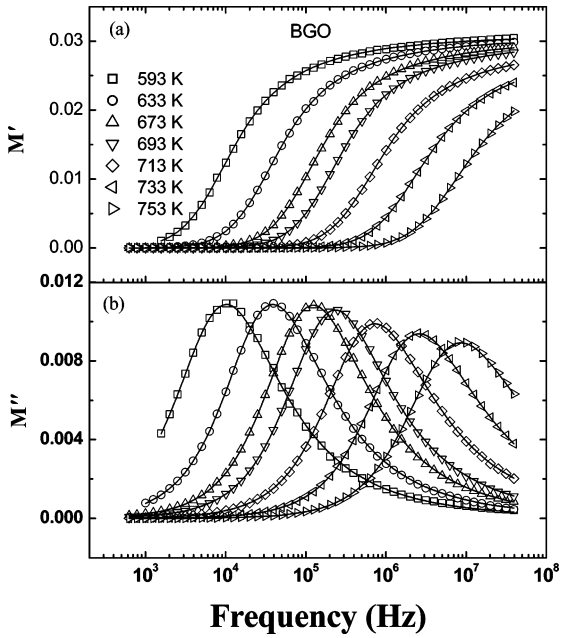

Figure 1. Angular frequency spectra of (a) the real and (b) the imaginary parts of the electric modulus for BGO glass at several temperatures. The solid curves are the best fits to eq 2 with LEVM, which is the particular complex nonlinear least-squares fitting program.

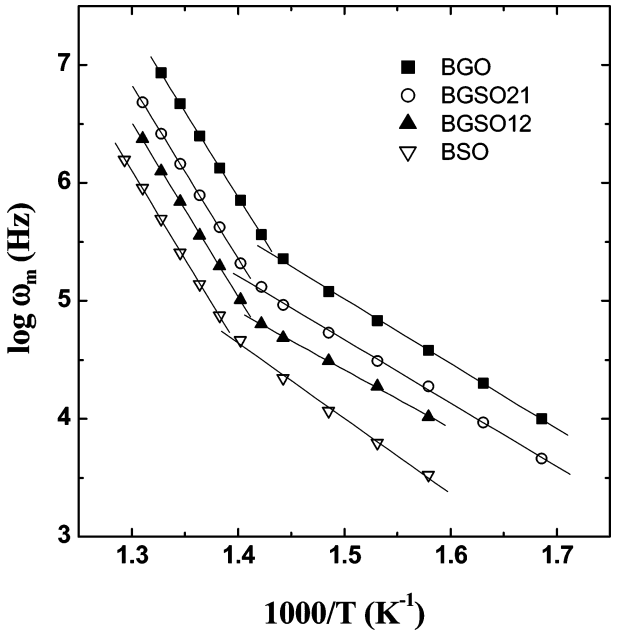

Figure 2. Temperature dependence of the peak frequency for different compositions of BGSO glasses, obtained from the fits of the complex modulus formalism. The solid lines are the least-squares straight-line fits to data. The glass transition temperatures of BGO, BGSO21, BGSO12, and BSO are 703, 707, 710, and 721 K, respectively.

Boltzmann constant. The slopes of the least-squares straight-line fits represent the values of activation energy for different compositions of BGSO glasses. Correspondingly, the activation energies, E_m, of the BGO, BGSO21, BGSO12, and BSO are 1.11, 1.07, 0.98, and 1.27 eV below T_g and 2.85, 2.92, 2.93, and 2.96 eV above T_g, respectively. The glass transition temperature T_g is the point of the slope change for each composition.

The complex modulus activation energy E_m obtained from the slopes in Figure 2 was close to not only the complex impedance activation energy E_{dc} of the Cole−Cole analysis but also the power-law dc activation energy E'_{dc} of the hopping

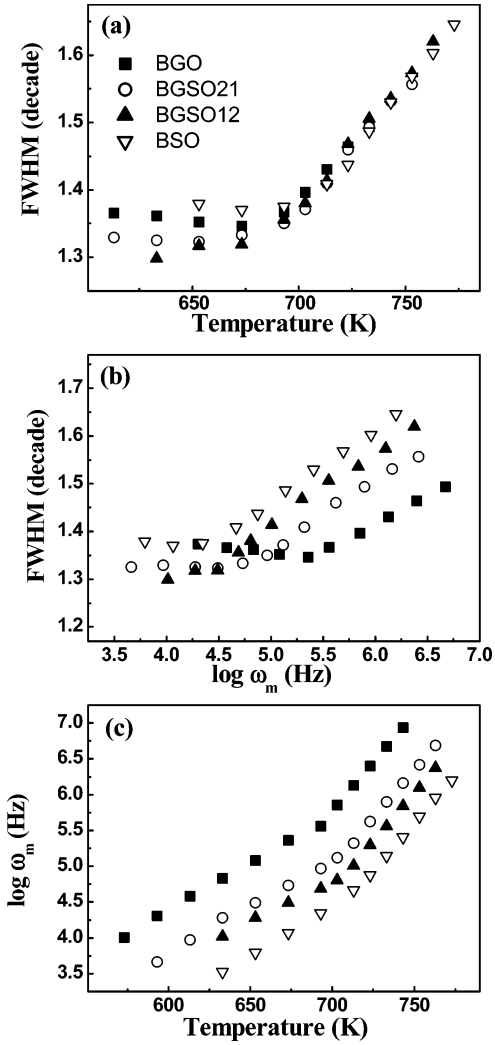

Figure 3. (a) Composition dependence of the fwhm at various temperatures. (b) Composition dependence of the fwhm at various peak frequencies. (c) Composition dependence of the peak frequency at various temperatures. The full width at half-maximum of $M''(\omega)$ normalized by the Debye width for different compositions of BGSO samples. The fwhm's were obtained by the best fit of the experimental curves from the frequency dependence of $M''(\omega)$.

carrier in the whole range of the experimental temperature, which had been obtained in a previous paper.[11] It is customary to associate with σ_{dc} a frequency scale, $\sigma_{dc} = \epsilon_0\epsilon_\infty/\langle\tau\rangle = \omega_m\epsilon_0/M_\infty$,[26] where σ_{dc} is dc conductivity. This shows that the BGSO glasses not only in the conductivity representation but also in the modulus representation satisfy the BNN relation. Since the BNN relation[27−29] implies $\omega_m \sim \sigma_{dc}$ or σ'_{dc}, while $\sigma_{dc} \propto \exp(-E_{dc}/kT)$, $\sigma'_{dc} \propto \exp(-E'_{dc}/kT)$, thus ω_m obey the Arrhenius relation. Therefore, we may draw the same conclusion in the modulus representation as in the conductivity representation that the dc conductivity decreases with an increase in Si content, representing the higher activation energy.[11]

From the frequency dependence of $M''(\omega)$ for various compositions of BGSO glasses at several different temperatures, we obtain the full width at half-maximum (fwhm) by the best fit of the experimental curves for BGSO glasses. In Figure 3, we present the dependence of the fwhm and the dielectric loss peak frequency of $M''(\omega)$ at various temperatures and compositions. The fwhm, Γ_Ω, is normalized by the width of a typical Debye characteristic 1.14 decades.

In Figure 3, we plot (a) Γ_Ω vs T, (b) log ω_m vs Γ_Ω, and (c) log ω_m vs T. The plot Γ_Ω vs T in Figure 3a shows that the normalized fwhm for BGSO glass is constant approximately below T_g but the fwhm increases with increasing temperature above T_g. The fwhm's of BGO and BSO broaden slightly (0.04 decades) compared with the fwhm's of BGSO below T_g, but the fwhm's of BGSO samples are independent of compositions for the temperature above T_g. The independence of fwhm's for compositions above T_g is a different result from the previous result of the conductivity representation.[11] The change of the fwhm of our samples may be due to the structural looseness and the interactions of mobile ions. That is, for increasing temperature, the interaction between conducting ions and surrounding ions decreases due to the loosened network below T_g but the interaction of mobile ions increases with a pronounced decrease in viscosity above T_g.[11]

The plot log ω_m vs Γ_Ω in Figure 3b shows the normalized fwhm of $M''(\omega)$ at various compositions as a function of the dielectric loss peak frequency ω_m of $M''(\omega)$. The fwhm of BGSO glass at given ω_m increases with increasing Si content above T_g. According to the results of the conductivity representation, the dc conductivity decreases with increasing Si content because of the increase of interaction between Bi and nonbridging oxygen. As mentioned in Figure 2, the BGSO glasses in the modulus representation satisfy the BNN relation. Therefore, the non-Debye characteristic behavior upon increasing the fwhm increases due to the increase of interaction between Bi and nonbridging oxygen above T_g.

The plot log ω_m vs T in Figure 3c, which is almost identical with that of Figure 2, shows that the position of ω_m increases with increasing temperature and with increasing Ge content. This indicates that the BGSO sample relaxes quickly for an external electric field at elevated temperature and at a higher concentration of germanate. In the conductivity representation, the composition-dependent activation energy decreases with an increase in compound of Ge over the whole range of experimental temperatures. Correspondingly, dc conductivity increases with an increase in Ge content. Again, this result is exactly the same as the one in the plot log ω_m vs Γ_Ω in Figure 3b except that it covers the whole range of the temperature.

Therefore, the non-Debye response of $M''(\omega)$ in BGSO samples is due to the structural looseness and instability but not necessarily proportional to the amount of cation concentrations above T_g especially.

The frequency dependence of $M'(\omega)$ and $M''(\omega)$ for various compositions of BGSO glasses at two different temperatures is shown in Figure 4. The unfilled symbols refer to the data below T_g, and the filled symbols refer to the data above T_g. The data for $M'(\omega)$ and $M''(\omega)$ in Figure 4 were fitted simultaneously to eq 2. The $M'(\omega)$ of the BGSO samples shows the dispersion at high frequency at two different temperatures of 653 and 753 K, since those data of $M'(\omega)$ do not approach to M'_∞. Similarly in Figure 3c, the peak position ω_m of $M''(\omega)$ shifts clearly to higher frequencies as the Ge content increases at a given temperature, indicating that the Ge content sample stabilizes in a short time for an external force compared with the Si content sample at the same temperature.

In Figure 5, we present the values of the stretched-exponential parameter β obtained from the fits to eq 2 with LEVM program[30] at various temperatures. The values of β may be obtained either by using LEVM, which is the particular complex nonlinear least-squares (CNLS) fitting program, or by using our analytical form of the solution for $M''(\omega)$ in the Appendix.

We note that the measured glass transition temperatures of BGO, BGSO21, BGSO12, and BSO are 703, 707, 710, and 721 K, respectively. As the Si content increases, T_g increases slightly. The value of β in Figure 5 may be proportional to the inverse of the fwhm in Figure 3.

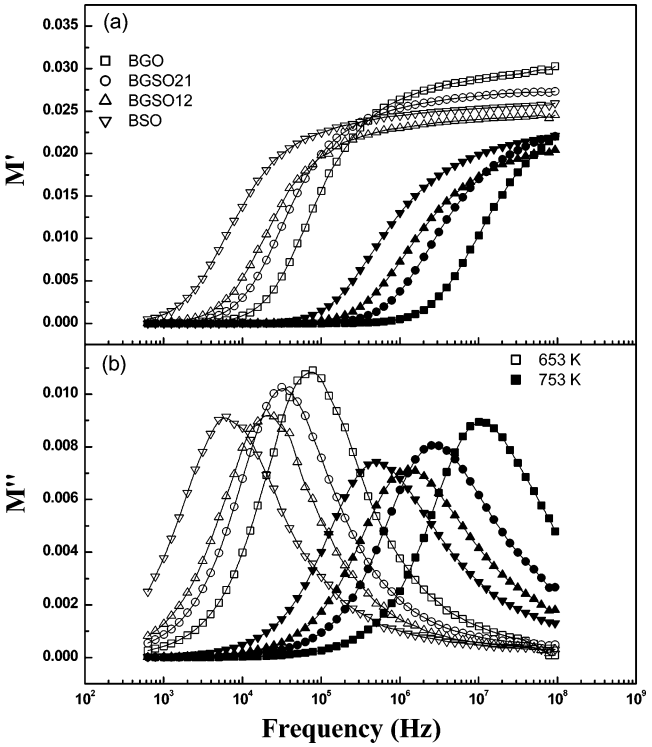

Figure 4. Frequency spectra of (a) the real and (b) the imaginary parts of the electric modulus for various compositions of BGSO glasses at two different sets of temperatures. The all open and all filled symbols stand for 653 and 753 K, respectively. The solid curves are the best fits to eq 2.

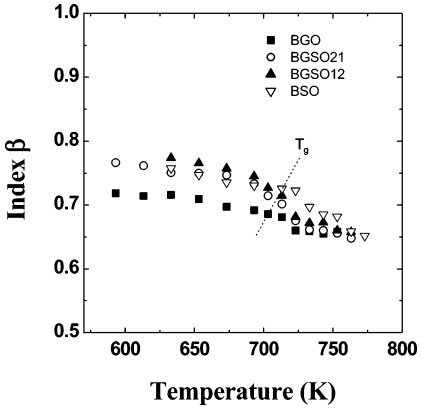

Figure 5. Temperature dependence of the stretched-exponential parameter obtained from the fits to eq 2 for different compositions of BGSO glasses. The glass transition temperatures of BGO, BGSO21, BGSO12, and BSO are 703, 707, 710, and 721 K, respectively.

As shown in Figure 5, the value of β of BGSO samples is constant approximately below T_g but it decreases rapidly in a short range of temperatures and then approaches a constant value for all compositions of the samples above T_g. Also, as the germanium content increases, the stretched-exponent β decreases in the whole range of temperatures. This temperature dependence of β may be due to the fact that the motion of the cation is dominant through the nonbridging oxygen from the loosened glass network below T_g, but the increasing interaction among thermally activated mobile ions such as Bi, Ge, and Si above T_g increases the non-Debye behavior of the samples.

In general, the non-Debye characteristic increases with the decreasing value of β. Although β is not a simple parameter to determine conductivity, the relationship can be deduced from the fact that the dc conductivity changes with β, since, from the results of Figures 3 and 5, the dc conductivity increases if the fwhm increases or the value of β decreases, even though the value of β of BGO sample is smaller than the one of BGSO samples below T_g but the dc conductivity increases with increasing Ge content. As we mentioned in Figure 3, the BGSO sample relaxes quickly for an external electric field not only at elevated temperature but also at a higher concentration of germanate. The rapid relaxation of the BGO sample for an external field may be the reason for increasing the non-Debye behavior without reducing the interaction of cation and nonbridging oxygen in BGSO samples below T_g.

B. Comparison with Power-Law Conductivity Data. The alternative representation of the macroscopic conductivity, $\sigma^*_{EM}(\omega)$, obtained from the electric modulus formalism via the Maxwell relation can be rewritten as the following[31]

$$\sigma^*_{EM}(\omega) = i\omega\epsilon_0/M^*(\omega) = (i\omega)(\epsilon_0/M_\infty)\{1/[1 - \int_0^\infty dt \exp(-i\omega t)(-d\phi(t)/dt)]\} \quad (5)$$

The real part of $\sigma^*_{EM}(\omega)$, given by the bulk frequency-dependent conductivity $\sigma(\omega)$ from the movement of dissociated cations in the glass matrix, is described by

$$\sigma(\omega) = \sigma'_{dc}[1 + (\omega/\omega_{ac})^n] \quad (6)$$

where σ'_{dc} is the dc conductivity from the power-law fit, ω_{ac} is the ionic hopping rate, and n is a frequency exponent parameter in the range $0 \le n \le 1$ characterizing the deviation from Debye behavior and measuring of the interionic coupling strength.[32−34] In the conductivity representation, the values of parameter n decreased with increasing temperature below T_g but showed an increasing trend with increasing content of germanium above T_g. The temperature dependence of n was understood in that the looseness of the glass network increased with increasing temperature and the interactions between conducting ions and surrounding decreased below T_g. The stronger interaction of the cation in BSO is expected by the higher density of nonbridging oxygen from the loosened glass network, compared with that of BGO below T_g. While, in the supercooled liquid state, above T_g, a high value of n in BGO may be due to the fact that there is a chance for mobile ions to interact with other atoms with a pronounced decrease in viscosity.[11] As we mentioned in Figure 5, again, the value of β of BGSO samples is constant approximately below T_g but it decreases rapidly in a short range of temperatures and then approaches constant value for all compositions of the samples above T_g. Also, as the germanium content increases, the stretched-exponent β decreases in the whole range of temperatures. Thus, the characteristics of n and β below T_g turned out to be consistent regarding the interactions but their characteristics above T_g are inconsistent.

Here, one must integrate eq 2 for $M^*(\omega)$ with the time evolution function $\phi(t)$ from eq 3 to obtain a proper relation between the exponents n and β by solving the integral in the Appendix of the form as following[35]

$$I = \int_0^\infty x^{\beta-1} \exp(-x^\beta)(-\cos \tau_k\omega x + i \sin \tau_k\omega x)\, dx \quad (7)$$

where $x = t/\tau_k$.

Since the first term in eqs A2 and A3 is not dominant in the series expansion, we have to consider whole expression in eqs A2 and A3 to find the exact relation between n and β. This is very complicated and tedious. However, considering the first and second terms in eqs A2 and A3 as an approximation, then we may have the following explicit relation between n and β from eqs 6 and A4

$$\sigma'_{dc}[1+(\omega/\omega_{ac})^n] \cong \frac{\epsilon_0\omega\beta}{M_\infty} \times \frac{\left[C'_1\left(\frac{\tau_k\omega}{2}\right)^{-\beta} - C'_2\left(\frac{\tau_k\omega}{2}\right)^{-2\beta}\right]}{\left[1-2\beta C_1\left(\frac{\tau_k\omega}{2}\right)^{-\beta} + (2\beta C_2+\beta^2 C_3)\left(\frac{\tau_k\omega}{2}\right)^{-2\beta} + \Theta((\tau_k\omega)^{-3\beta})\right]} \quad (8)$$

where τ_k is the KWW relaxation time related to the mean electric field relaxation time, C_1, C_2, C'_1, and C'_2 are constants of the order of 10^{-1}, $C_3 = C_1^2 + C_1'^2$, and $\Theta((\tau_k\omega)^{-3\beta})$ is the higher order term in the expansion.

In the limit of the high-frequency ($\tau_k\omega \gg 1$), the first term in the numerator is dominant and we have $n + \beta = 1$. However, the relation of $n + \beta = 1$ does not hold for other ranges of frequency. In contrast to our result, in the jump relaxation model, the exponents n and β turn out to add up to one in the power-law ac conductivity regime,[8] that is, $n + \beta = 1$. In the power-law regime, the behavior of $\beta(T)$ is quite different with the case of the frequency exponent $n(T)$ in the power-law conductivity representation in the BGSO samples especially. To find the proper relation between n and β in general, we may have to consider the whole expression in eqs A2 and A3 or we may use the approximate expression of eq 8.

To test the legitimacy of the analytical solution of $M''(\omega)$ in the Appendix, we performed the numerical calculation by choosing particular numbers of $0.6 < \beta < 0.8$ from the data in Figure 5. That is, we choose the numbers of β ($= 2p/q$) such as $10/13 = 0.77$, $26/37 = 0.70$, $2/3 = 0.67$, $32/49 = 0.65$, and $26/41 = 0.63$ and take an appropriate characteristic relaxation time τ^* satisfying the condition $\tau^*\omega \approx 1$ similar to the case of $\tau_k\omega \approx 1$ in the LEVM program for the given sample. In Figure 6, we obtain the best fit of the experimental curves for the BGO glass at 653 and 753 K corresponding to $\beta = 0.70$ and $\beta = 0.65$, respectively, by taking $\tau^* = (1/16)\tau_k$, where $\tau_k \approx 1/\omega_m$. The solid and dotted lines represent the best fit with $\beta = 0.65$ and $\beta = 0.70$, respectively. The broadening tendency of the fwhm may be seen for decreasing β, but there is a discrepancy for fitting the data above T_g, curiously.

C. Scaling Relations. A master plot for the electric modulus $M^*(\omega)$ of BGSO samples is shown in Figure 6 at various compositions and temperatures. The shape of $M''(\omega)$ overlaps very well below and above T_g, but it broadens appreciably with increasing temperature. This result indicates that the dynamical processes are temperature dependent. However, the curves are overlapped into a single master curve for all the concentrations and at a given temperature. Thus, appropriate scaling results in a master curve suggest that the ionic relaxation mechanism in the BGSO sample is temperature dependent but it is concentration independent.

In the literature, the modulus of the ionic glass former $0.4Ca(NO_3)_2-0.6KNO_3$ (CKN) in the melt above T_g shows substantial broadening with increasing temperature.[26] This change of the spectrum with temperature is known due to the increased coupling of the ionic hopping relaxation with the structural relaxation upon increasing temperature,[26] while the shape of $M''(\omega)$ for the lithium tellurite glasses overlaps perfectly into a single master curve for all temperatures. Consequently, the dynamical processes of the lithium tellurite glasses are temperature independent.[36] The modulus of the alkali-oxide glasses exhibits substantial narrowing with decreasing ion concentration, which is caused by a weakening of the ion−ion interaction.[26,37−40]

In Figure 7, we present the ac conductivity in BGSO glasses at four compositions and two temperatures scaled using ω_{ac}. Sidebottom et al. chose an appropriate scaling factor

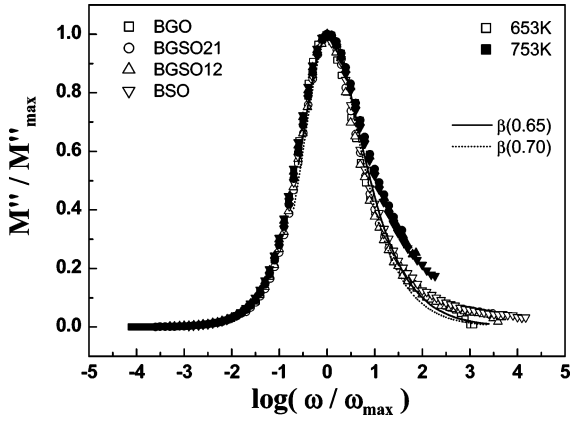

Figure 6. Plot of M''/M''_{max} vs $\log(\omega/\omega_{max})$ for various compositions of BGSO glasses at two different sets of temperatures. The unfilled symbols refer to the data at 653 K below T_g, and the filled symbols refer to the data at 753 K above T_g. The solid and dotted lines represent the best fits to the analytical expression of $M''(\omega)$ in eqs A1 and A3 with $\beta = 0.65$ at 753 K and $\beta = 0.70$ at 653 K, respectively.

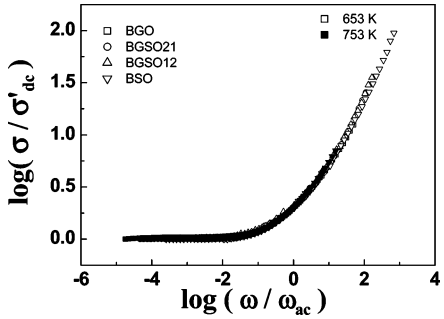

Figure 7. Plot of $\log(\sigma/\sigma'_{dc})$ vs $\log(\omega/\omega_{max})$ for various compositions of BGSO glasses at two different sets of temperatures. The unfilled symbols refer to the data at 653 K below T_g, and the filled symbols refer to the data at 753 K above T_g.

$\omega_0 = 2\pi\sigma'_{dc}/(\epsilon_0\Delta\epsilon)$ for potassium thioborate glasses.[37,41,42] As pointed out in a letter,[41] the scaling factor ω_0 is related to the frequency of maximum dielectric loss ω_m in the complex impedance analysis.[11] Curiously, the characteristic frequency ω_0 has the same value as ω_{ac} which is obtained by Jonscher's power-law method in the conductivity representation of BGSO glasses, that is, $\omega_0 \cong \omega_{ac}$. The crossover frequency from the dc behavior to the dispersive conductivity, ω_{ac}, is defined by $\sigma(\omega_{ac}) = 2\sigma'_{dc}$ in eq 6. As shown in Yang et al.,[11] ω_{ac} contains various parameters such as $x/(\sigma'_{dc}T)$, with $\Delta\epsilon$ implicitly through the corresponding activation energy of the BGSO samples. Here, x is the concentration of the germanium oxide content in the BGSO glasses, and $\Delta\epsilon$ is the permittivity change of the samples. It is worthwhile to note that the expression of the permittivity change of the BGSO samples is determined by the distribution of relaxation times, which is proposed by Ngai et al. and expressed as $\Delta\epsilon = [\beta(\Gamma(2/\beta)/[\Gamma(1/\beta)]^2) - 1]\epsilon_\infty$.[26]

Moreover, the scaling factor ω_0 is a good choice for the characteristic peak frequency ω_m of the modulus representation of BGSO glasses again, since the typical characteristic frequencies obtained from the experiment are $\omega_0 \cong 2.8$ MHz $\omega_{ac} \cong 2.5$ MHz, and $\omega_m \cong 2.5$ MHz at $T = 733$ K for the BGO sample.

IV. Conclusions

The complex modulus and the power-law methods are adapted for the analysis of the electrical conductivities of BGSO glasses.

The complex modulus activation energy E_m obeys the Arrhenius relation, and consequently, the BGSO glasses satisfy

the BNN relation, which is the consistent result of the power-law conductivity in the conductivity representation.

The characteristics of ionic conductivity and the non-Debye response of $M''(\omega)$ in BGSO samples are due to the structural looseness and instability rather than the change of the concentrations of the mobile ions. In the sense of the interactions, the characteristics of n and β turned out to be consistent below T_g but their characteristics above T_g are inconsistent.

In contrast to the result of the jump relaxation model, the exponents n and β do not turn out to add up to one in the power-law ac conductivity regime for the BGSO samples.

The numerical calculation of our analytical expression of $M''(\omega)$ confirms the legitimacy to fit the experimental curves for the modulus representation.

The scaling results show that the ionic relaxation mechanism in the BGSO sample is temperature dependent and concentration independent.

The choice of scaling factor ω_0 is appropriated both of the ac conductivity representation and of the modulus representation in BGSO glasses.

Acknowledgment. This work was supported in part by the Semyung University 2005 Research Grant for Y.H.R. This research was supported by the Program for the Training of Graduate Students in Regional Innovation, which was conducted by the Ministry of Commerce, Industry and Energy of the Korean Government, and by a Korea Research Foundation Grant (KRF-2004-005-C00041).

Appendix

The complex electric modulus $M^*(\omega)$ in eq 2 with the KWW function can be rewritten as

$$M^*(\omega) = M_\infty + M_\infty\beta\,[\int_0^\infty x^{\beta-1} \times \exp(-x^\beta)(\cos\tau_k\omega x)\,dx - i\int_0^\infty x^{\beta-1}\exp(-x^\beta)(\sin\tau_k\omega x)\,dx] \quad \text{(A1)}$$

where $x = t/\tau_k$.The relation between the macroscopic ac conductivity and the electric modulus formalism descriptions are summarized here as follows

$$I_1 = \int_0^\infty x^{\beta-1}\exp(-x^\beta)(\cos\tau_k\omega x)\,dx = \sum_{j=0}^{q-1}\frac{(-1)^j}{j!}\frac{\sqrt{\pi}}{2}\Gamma\begin{bmatrix}\beta(j+1)/2\\1/2-\beta(j+1)/2\end{bmatrix}(\tau_k\omega/2)^{-\beta(j+1)}\cdot {}_{2p+1}\mathbf{F}_q\begin{pmatrix}1,\Delta(p,\beta(j+1)/2),\Delta(p,\beta(j+1)/2+1/2);Z_2\\\Delta(q,1+j)\end{pmatrix} \quad \text{(A2)}$$

$$I_2 = \int_0^\infty x^{\beta-1}\exp(-x^\beta)(\sin\tau_k\omega x)\,dx = \sum_{j=0}^{q-1}\frac{(-1)^j}{j!}\frac{\sqrt{\pi}}{2}\Gamma\begin{bmatrix}\beta(j+1)/2+1/2\\1-\beta(j+1)/2\end{bmatrix}(\tau_k\omega/2)^{-\beta(j+1)}\cdot {}_{2p+1}\mathbf{F}_q\begin{pmatrix}1,\Delta(p,\beta(j+1)/2+1/2),\Delta(p,\beta(j+1)/2);Z_2\\\Delta(q,1+j)\end{pmatrix} \quad \text{(A3)}$$

and

$$\Gamma\begin{bmatrix}a_1,\ldots,a_m\\b_1,\ldots,b_n\end{bmatrix} = \frac{\prod_{k=1}^{m}\Gamma(a_k)}{\prod_{l=1}^{n}\Gamma(b_l)},\ {}_p\mathbf{F}_q\begin{pmatrix}a_1,\ldots,a_p;Z\\b_1,\ldots,b_q\end{pmatrix}$$

is the generalized hypergeometric function, $\Delta(k,a) = a/k$, $(a+1)/k$, ..., $(a+k-1)/k$, $Z_2 = (-1)^{p+q}(\tau_k\omega/2p)^{-2p}q^{-q}$, $\beta/2 = p/q$, and p, q are relatively prime numbers.

From eqs 5, A1, A2, and A3, we have

$$\mathrm{Re}\,\sigma^*_{EM}(\omega) = \frac{\epsilon_0\omega}{M_\infty}\frac{\beta I_2}{(1-\beta I_1)^2+(\beta I_2)^2} \quad \text{(A4)}$$

References and Notes

(1) Link, J.; Fontanella, J. *J. Appl. Phys.* **1980**, *51*, 4352.
(2) Schweppe, H. *IEEE Trans. Sonics Ultrason.* **1969**, *SU-16*, 219.
(3) Moncorge, R.; Jacquier, B.; Boulon, G. *J. Lumin.* **1976**, *14*, 337.
(4) Angell, C. A. *Chem. Rev.* **1990**, *90*, 523.
(5) Elliott, S. R.; Owen, A. P. *Ber. Bunsen-Ges., Phys. Chem.* **1991**, *95*, 987.
(6) Bunde, A.; Ingram, M. D.; Maass, P. *J. Non-Cryst. Solids* **1994**, *172−174*, 1222.
(7) Sidebottom, D. L.; Green, P. F.; Brow, R. K. *J. Chem. Phys.* **1998**, *108*, 5870.
(8) Funke, K. *Prog. Solid State Chem.* **1993**, *22*, 111.
(9) Maass, P.; Meyer, M.; Bunde, A. *Phys. Rev. B* **1995**, *51*, 8164.
(10) Ngai, K. L. *J. Non-Cryst. Solids* **1996**, *103*, 232.
(11) Yang, Y. S.; Cho, J. H.; Kim, S. J.; Kim, J. E.; Choi, H. W.; Rim, Y. H. *J. Phys. Chem. B* **2004**, *108*, 16659.
(12) Cho, J. H.; Kim, S. K.; Yang, Y. S. *Solid State Commun.* **2001**, *119*, 465.
(13) Havriliak, S.; Negami, S. *J. Polym. Sci., Part C: Polym. Lett.* **1996**, *9*, 99.
(14) Feldman, Y.; Puzenko, A.; Ryabov, Y. *Chem. Phys.* **2002**, *284*, 139.
(15) Dieterich, W.; Maass, P. *Chem. Phys.* **2002**, *284*, 439.
(16) Metzler, R.; Klafter, J. *J. Non-Cryst. Solids* **2002**, *305*, 81.
(17) Nonnenmacher, T. F.; Glöckle, W. G. *Philos. Mag. Lett.* **1991**, *64*, 89. Nonnenmacher, T. F. *Rheological Modeling: Thermodynamical and Statistical Approaches, Lecture Notes in Physics*; Casas-Vázquez, J., Jou, D., Eds.; Springer: Berlin, 1991; Vol. 381.
(18) Sokolov, I. M.; Klafter, J.; Blumen, A. *Phys. Today* **2002**, *55*, 48.
(19) Kalmykov, Y. P.; Coffey, W. T.; Titov, S. V. *Phys. Rev. E* **2004**, *69*, 021105.
(20) Moynihan, C. T.; Boesch, L. P.; Laberge, N. L. *Phys. Chem. Glasses* **1973**, *14*, 122.
(21) Provenzano, V.; Boesch, L. P.; Volterra, V.; Moynihan, C. T.; Macedo, P. B. *J. Am. Ceram. Soc.* **1972**, *55*, 492.
(22) Macedo, P. B.; Moynihan, C. T.; Bose, R. *Phys. Chem. Glasses* **1972**, *13*, 171.
(23) Howell, F. S.; Bose, R. A.; Macedo, P. B.; Moynihan, C. T. *J. Phys. Chem.* **1974**, *78*, 639.
(24) Kohlrausch, R. *Ann. Phys.* (Leipzig) **1847**, *12*, 393.
(25) Williams, G.; Watts, D. C. *Trans. Faraday Soc.* **1970**, *66*, 80.
(26) Ngai, K. L.; Rendell, R. W. *Phys. Rev. B* **2000**, *61*, 9393.
(27) Barton, J. L. *Verres Réfract.* **1996**, *20*, 328.
(28) Nakajima, T. In *1971 Annual Report, Conference on Electric Insulation and Dielectric Phenomena*; National Academy of Sciences: Washington, DC, 1972; p 168.
(29) Namikawa, H. *J. Non-Cryst. Solids* **1975**, *18*, 173.
(30) Macdonald, R. *CNLS Immittance, Inversion, and Simulation Fitting Programs for WINDOWS and MS-DOS LEVM Manual*; J. Ross Macdonald and Solartron Limited, 1999−2003.
(31) Ngai, K. L.; León, C. *Phys. Rev. B* **1999**, *60*, 9396.
(32) Ngai, K. L.; Rendell, R. W.; Jain, H. *Phys. Rev. B* **1984**, *30*, 2133.
(33) Ngai, K. L.; Mundy, J. N.; Jain, H.; Kannert, O.; Balzer-Jollenbeck, G. *Phys. Rev. B* **1989**, *39*, 6169.
(34) Kannert, O.; Steinert, J.; Jain, H.; Ngai, K. L. *J. Non-Cryst. Solids* **1991**, *131*, 1001.
(35) Prudnikov, A. P.; Brychkov, Yu. A.; Marichev, O. I. *Integrals and Series*; Gordon and Breach Science Publishers: New York, 1986; Vol. 1, p 382.
(36) Pan, A.; Ghosh, A. *Phys. Rev. B* **1999**, *60*, 3224.
(37) Patel, H. K. Ph.D. Thesis, Iowa State University, Ames, Iowa, 1993.
(38) Sidebottom, D. L.; Green, P. F.; Brow, R. K. *Phys. Rev. B* **1997**, *56*, 170.
(39) Patel, H. K.; Martin, S. W. *Phys. Rev. B* **1992**, *45*, 10292.
(40) Patel, H. K.; Martin, S. W. *Solid State Ionics* **1992**, *53−54*, 1148.
(41) Sidebottom, D. L. *Phys. Rev. Lett.* **1999**, *82*, 3653.
(42) Schroder, T. B.; Dyre, J. C. *Phys. Rev. Lett.* **2000**, *84*, 310.